FEBS Letters 588 (2014) 389–394

journal homepage: www.FEBSLetters.org

The extreme N-terminal region of human apolipoprotein A-I has a strong propensity to form amyloid fibrils

Emi Adachi [a], Asako Kosaka [a], Kohei Tsuji [a], Chiharu Mizuguchi [a], Hiroyuki Kawashima [b], Akira Shigenaga [a], Kohjiro Nagao [a], Kenichi Akaji [b], Akira Otaka [a], Hiroyuki Saito [a,*]

[a] Institute of Health Biosciences and Graduate School of Pharmaceutical Sciences, The University of Tokushima, 1-78-1 Shomachi, Tokushima 770-8505, Japan
[b] Department of Medicinal Chemistry, Kyoto Pharmaceutical University, Yamashina-ku, Kyoto 607-8412, Japan

ARTICLE INFO

Article history:
Received 27 August 2013
Revised 10 November 2013
Accepted 25 November 2013
Available online 5 December 2013

Edited by Jesus Avila

Keywords:
Apolipoprotein A-I
Amyloid fibril
Peptide
Point mutation

ABSTRACT

The N-terminal 1–83 residues of apolipoprotein A-I (apoA-I) have a strong propensity to form amyloid fibrils, in which the 46–59 segment was reported to aggregate to form amyloid-like fibrils. In this study, we demonstrated that a fragment peptide comprising the extreme N-terminal 1–43 residues strongly forms amyloid fibrils with a transition to β-sheet-rich structure, and that the G26R point mutation enhances the fibril formation of this segment. Our results suggest that in addition to the 46–59 segment, the extreme N-terminal region plays a crucial role in the development of amyloid fibrils by the N-terminal fragment of amyloidogenic apoA-I variants.

Structured summary of protein interactions:
apoA-I and **apoA-I** bind by fluorescence technology (1, 2, 3)
apoA-I and **apoA-I** bind by atomic force microscopy (View interaction)
apoA-I and **apoA-I** bind by dynamic light scattering (1, 2)

1. Introduction

Apolipoprotein A-I (apoA-I) is the major protein component of plasma high-density lipoprotein (HDL) and plays a central role in reverse cholesterol transport [1,2]. Naturally occurring mutations in human apoA-I are known to affect its functionality mainly in two ways: mutations in the N terminus of residues 1–90 are associated with hereditary amyloidosis, whereas those within the central region of residues 140–170 are mostly associated with defective activation of lecithin-cholesterol acyltransferase [3,4]. In addition to the 1–90 region, a number of amyloidogenic variants are also found in residues 170–180 [5,6]. In most hereditary amyloidogenic mutations, the N-terminal fragment of mutated apoA-I is the predominant form of protein found in amyloid fibril deposits [7,8], suggesting that the N-terminal region is critical to the amyloid fibril formation of apoA-I [9]. Consistent with this, we recently found that the N-terminal 1–83 fragment of apoA-I has a strong propensity to form amyloid fibrils at neutral pH, and that the G26R point mutation, the first amyloidogenic mutation found in apoA-I [10], greatly enhances the amyloid fibril formation of this N-terminal fragment [11].

Non-hereditary forms of wild-type apoA-I are also commonly observed to be deposited as amyloid fibrils in atherosclerotic plaques [12], suggesting that mutations in the protein are not essential for its conversion into amyloid [13]. Prediction of the β-aggregation propensity of the N-terminal region in apoA-I based on amino acid sequence [14] indicates that residues 14–22 and 49–57 are the most aggregation prone segments [9]. In fact, a peptide comprising residues 46–59 of apoA-I was shown to form amyloid fibrils with cross-β structure [15], consistent with the possibility that segment 44–55 can provide a template for the formation of an intermolecular β-sheet in fibrils [16].

In the present study, we examined the aggregation propensity of three regions of the N-terminal 1–83 fragment, residues 1–43, 44–65, and 66–83 using synthetic fragment peptides. Residues 1–43 which are encoded by exon 3 were shown to contribute to the lipid-free conformation and lipid interaction of apoA-I [17,18]. Residues 44–65 are the first amphipathic α-helical repeat which has high lipid affinity [19] and contain the reported amyloid fibril-forming region of residues 46–59 [15]. The results

Abbreviations: AFM, atomic force microscopy; apoA-I, apolipoprotein A-I; ATR, attenuated total reflection; FTIR, fourier transform infrared spectroscopy; HDL, high-density lipoprotein; ThT, thioflavinT; WMF, wavelength of maximum fluorescence

* Corresponding author. Fax: +81 88 633 9510.
E-mail address: hsaito@tokushima-u.ac.jp (H. Saito).

0014-5793/$36.00
http://dx.doi.org/10.1016/j.febslet.2013.11.031

demonstrated that in addition to the 46–59 segment, the extreme N-terminal 1–43 segment has a strong ability to form amyloid fibrils with a transition to β-sheet-rich structure, and that the G26R point mutation enhances the fibril formation of this segment.

2. Materials and methods

2.1. Peptide synthesis

ApoA-I peptides were synthesized on a 0.2 mmol scale using Fmoc chemistry. The N- and the C termini were capped with an acetyl group and an amide group, respectively. Peptides were cleaved from the resin using standard trifluoroacetic acid methods and purified by high-performance liquid chromatography and mass spectrometry. In all experiments, peptides were freshly dialyzed from 6 M guanidine hydrochloride solution into the appropriate buffer before use.

2.2. Fluorescence measurements

Kinetics of protein aggregation and fibril formation were monitored using fluorescent dyes, thioflavinT (ThT) and 8-anilino-1-naphthalenesulfonic acid (ANS). ApoA-I peptides (0.05–0.3 mg/ml) in 10 mM Tris buffer (150 mM NaCl, 0.02% NaN_3, pH 7.4) were incubated at 37 °C with agitation in the presence of 10 μM ThT or 10 μM ANS. The fluorescence of ThT or ANS was recorded by using an f_{max} fluorescence plate reader (Molecular Devices) with excitation and emission wavelengths of 445 and 485 nm for ThT or 395 and 495 nm for ANS, respectively. Trp fluorescence measurements were carried out with a Hitachi F-4500 fluorescence spectrophotometer. To assess the local environment of apoA-I peptides, Trp emission fluorescence was recorded from 300 to 420 nm using a 290 nm excitation wavelength to avoid tyrosine fluorescence. In quenching experiments of Trp fluorescence, Trp emission spectra of peptides were recorded at increasing concentrations of KI (0–0.56 M) using a 5 M stock solution containing 1 mM NaS_2O_3 to prevent the formation of iodine. After correction for dilution, the integrated fluorescence intensities were plotted according to the Stern–Volmer equation, $F_0/F = 1 + K_{sv}$ [KI], where F_0 and F are the fluorescence intensities in the absence and presence of quencher, respectively, and K_{sv} is the Stern–Volmer constant.

2.3. Atomic force microscopy (AFM)

For analysis by AFM, 10 μl of each peptide solution (0.1 mg/ml) in 10 mM Tris buffer was deposited on freshly cleaved mica (The Nilaco Corp., Tokyo, Japan). After washing the mica with distilled water (20 μl), samples were imaged under ambient conditions at room temperature using a NanoScope® IIIa tapping mode AFM (Veeco, Plainview, NY) and microcantilever OMCLAC160TS-R3 (Olympus, Tokyo, Japan).

2.4. Attenuated total reflection-Fourier transform infrared (ATR-FTIR) spectroscopy

ATR-FTIR spectra were recorded on a Jasco FTIR spectrometer FT/IR-6200 equipped with an ATR PRO610P-S reflectance accessory. An aliquot of peptide sample (0.1 mg/ml) in 10 mM Tris buffer (pH 7.4) was spread on the germanium waveguide, and the excess water was removed under nitrogen flow. ATR-FTIR spectra were recorded over the wave number range of 1000–3500 cm^{-1} at a resolution of 2 cm^{-1} and 256 accumulations under continuous nitrogen purge. To evaluate secondary structure, the amide I area (1600–1700 cm^{-1}) in the spectra was deconvoluted using a Spectra Manager Software (Jasco, Tokyo, Japan).

3. Results

3.1. Aggregation propensity of apoA-I N-terminal peptides

We first investigated the fibril-forming propensity of apoA-I 1–43, 44–65, and 66–83 peptides by monitoring the increase in ThT fluorescence, which is highly characteristic of amyloid fibril structure [20]. As shown in Fig. 1A, the 1–43 peptide exhibited large increases in ThT fluorescence on incubation at physiological conditions (pH 7.4 and 37 °C). The 44–65 peptide showed a relatively small but significant increase in ThT fluorescence, while almost no change in ThT fluorescence was observed for the 66–83

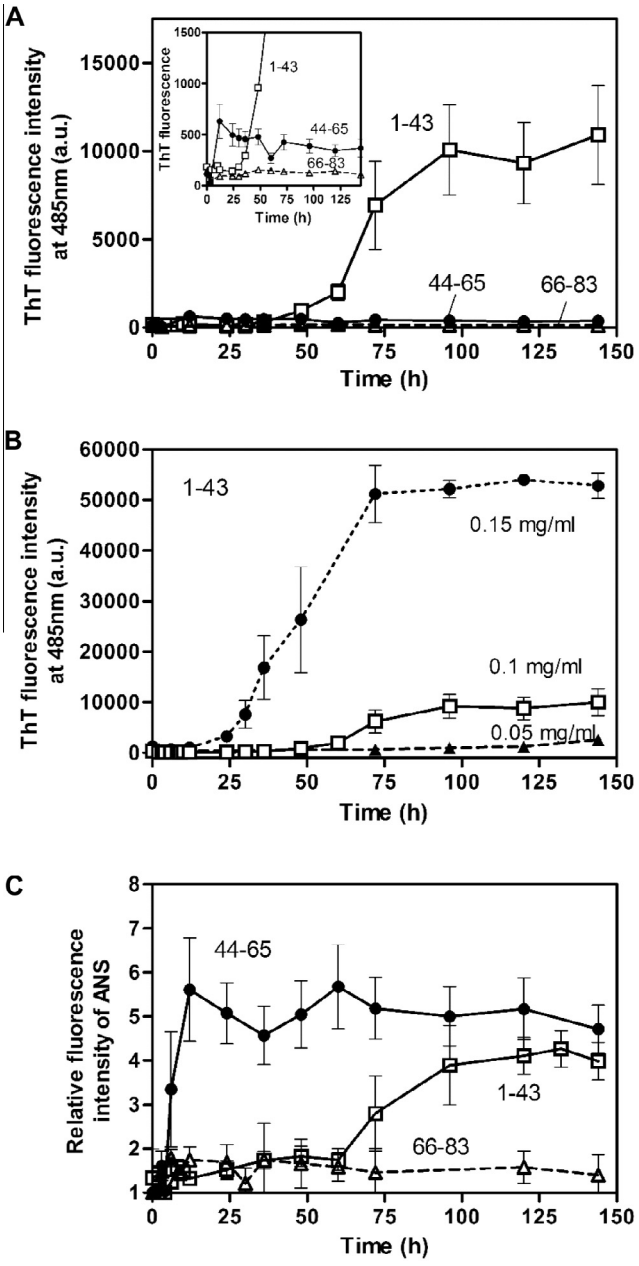

Fig. 1. Amyloid fibril formation of apoA-I peptides. (A) Fibril formation was monitored by ThT fluorescence for apoA-I 1–43 (□), 44–65 (●), and 66–83 (△) peptides incubated at pH 7.4. The inset shows an enlarged view. Peptide and ThT concentrations were 0.1 mg/ml and 10 μM, respectively. (B) Effect of peptide concentration on ThT fluorescence of apoA-I 1–43 peptide. ▲, 0.05 mg/ml; □, 0.1 mg/ml; ●, 0.15 mg/ml. (C) Change in ANS fluorescence for apoA-I 1–43 (□), 44–65 (●), and 66–83 (△) peptides over incubation time at pH 7.4. Peptide and ANS concentrations were 0.1 mg/ml and 10 μM, respectively.

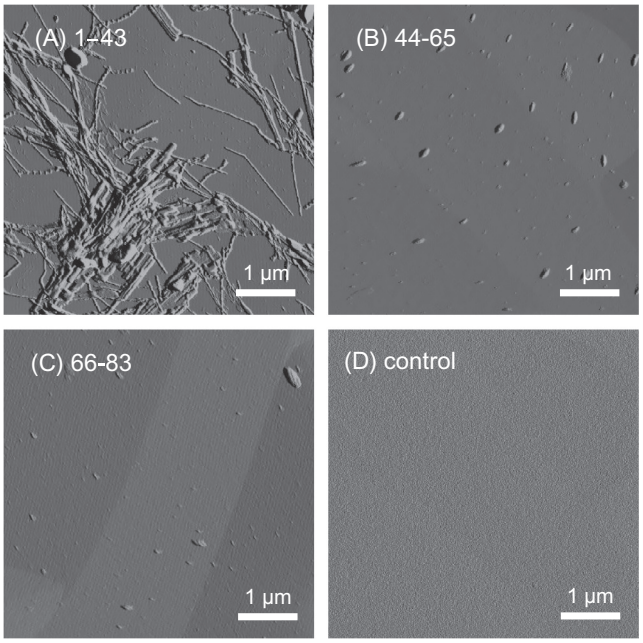

Fig. 2. AFM images of apoA-I 1–43 (A), 44–65 (B), and 66–83 (C) peptides after 144 h incubation at pH 7.4. Control image without peptide (D) is also shown for comparison. Scale bars represent 1 μm.

peptide. With increasing peptide concentration, the development of ThT fluorescence was significantly accelerated in apoA-I 1–43 (Fig. 1B) and 44–65 (Supplementary Fig. S1) peptides, indicating the strong fibrillogenic potential of both peptides. We also performed ANS binding studies to the apoA-I peptides to examine the aggregated state over incubation time because this dye binds to the fibrillar or prefibrillar aggregate states of proteins [21,22]. As shown in Fig. 1C, the 1–43 peptide exhibited significant increases in ANS fluorescence with similar kinetics to the increase in ThT fluorescence. Interestingly, much faster and larger increase in ANS fluorescence was observed for the 44–65 peptide, indicating the strong tendency to aggregate to form fibrils of this peptide. It should be noted that such a rapid increase in ANS fluorescence of this peptide is unlikely due to its helix formation because the transition to β-structure was observed even at early period (6 h or 12 h). In contrast, no significant increase in ANS fluorescence was detected for the 66–83 peptide.

Fig. 2 shows typical AFM images of the apoA-I peptides after incubation (more AFM images are shown in Supplementary Fig. S2), confirming that the 1–43 peptide formed large amounts of straight fibrils (Fig. 2A). In contrast, the 44–65 and 66–83 peptides did not show apparent fibril formation, but small spherical aggregates or short rods were observed especially for the 44–65 peptide (Fig. 2B and C). Dynamic light scattering measurements demonstrated that the 1–43 and 44–65 peptides form large aggregates with an average diameter of over 1 μm after incubation whereas the 66–83 does not (Supplementary Fig. S3). These results indicate that in addition to the 44–65 peptide which contains the amyloidogenic core region of apoA-I [15], the 1–43 peptide has a strong propensity to form amyloid fibrils. In contrast, the 66–83 peptide does not have a propensity to form fibrils at physiological pH.

3.2. Trp fluorescence of apoA-I N-terminal peptides

Taking advantage of the fact that each apoA-I peptide contains one intrinsic Trp residue (Trp-8, Trp-50, or Trp-72 for the 1–43,

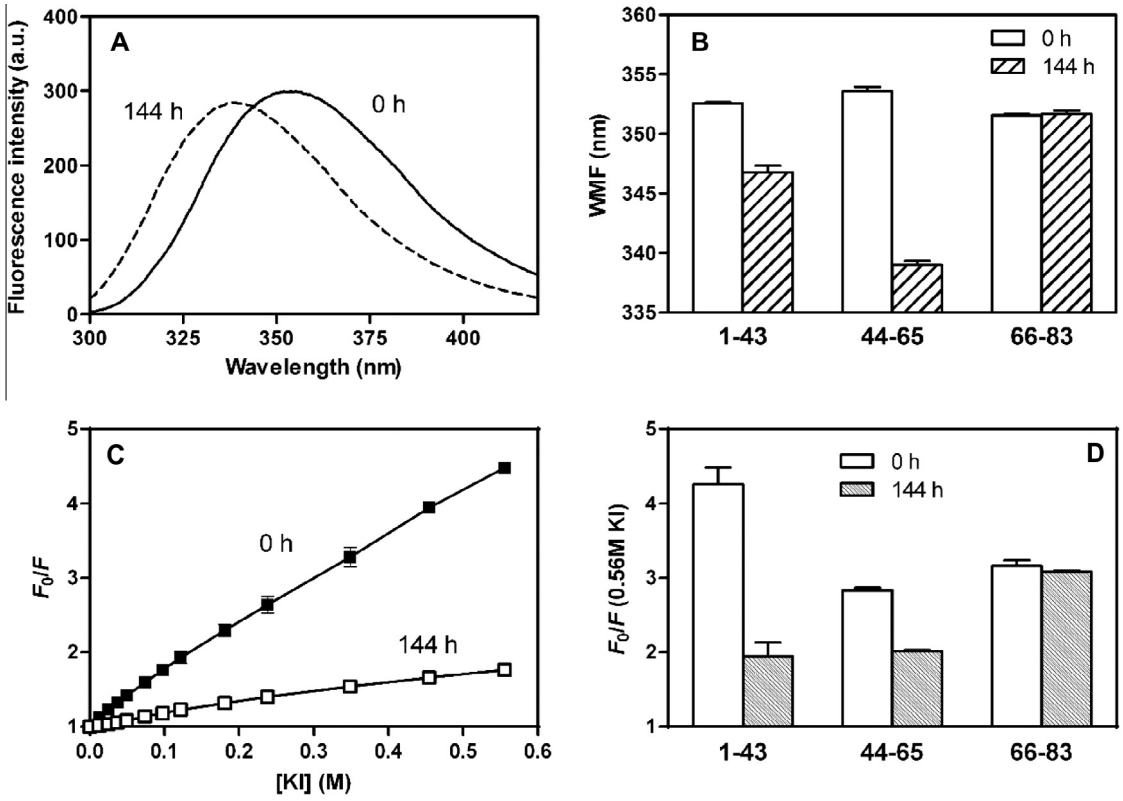

Fig. 3. Trp fluorescence of apoA-I peptides. (A) Trp fluorescence spectra of apoA-I 44–65 peptide (50 μg/ml) before (*solid line*) and after (*dashed line*) incubation for 144 h at pH 7.4. (B) Change in WMF of apoA-I peptides by the incubation. (C) Stern–Volmer plots for KI quenching of apoA-I 1–43 peptide before (■) and after (□) incubation for 144 h at pH 7.4. (D) Change in the quenching ratio at 0.56 M KI as a parameter of solvent accessibility for apoA-I peptides by the incubation.

44–65, or 66–83 peptides, respectively), we estimated the changes in local environment of the peptides along the aggregation time-courses using Trp fluorescence. Fig. 3A shows the Trp fluorescence emission spectra of the 44–65 peptide before and after incubation. A significant blue shift in wavelength of maximum fluorescence (WMF) after incubation indicates the transfer of Trp-50 into a more hydrophobic environment, reflecting a conformational transition of the 44–65 peptide with aggregation. Comparison of WMF among three apoA-I peptides (Fig. 3B) indicates that the 1–43 peptide underwent a similar change in conformation during aggregation, whereas the 66–83 peptide did not change conformation.

We also examined Trp quenching behavior of the three apoA-I peptides when exposed to the aqueous quencher KI before and after incubation. Stern–Volmer plots for the 1–43 peptide (Fig. 3C) indicate a great reduction of the solvent accessibility of Trp-8 after incubation, consistent with fibril formation of this peptide. Fig. 3D compares the quenching ratio at 0.56 M KI as a parameter of solvent accessibility for the three apoA-I peptides. Again, the 1–43 and 44–65 peptides exhibited a large reduction of the solvent accessibility after incubation, whereas no change was observed for the 66–83 peptide. These results are consistent with the notion that both the 1–43 and 44–65 segments contain aggregation core regions to form amyloid fibrils in their sequences whereas residues 66–83 do not.

3.3. Structural transition of apoA-I N-terminal peptides

To examine the secondary structural change in the apoA-I peptides, ATR-FTIR measurements were performed on the samples before and after incubation. Before incubation, the component at $\sim$1655 cm^{-1} was dominant in FTIR spectra for all three peptides (Fig. 4), implying the presence of α-helix or random-coil secondary structures [9]. After incubation, FTIR spectra of the 1–43 and 44–65 peptides showed that bands at $\sim$1630 cm^{-1} became evident (Fig. 4A and B), indicating the transition of these peptides to β-sheet structures [23]. In contrast, there was no change in FTIR spectra of the 66–83 peptide before and after incubation (Fig. 4C), consistent with residues 66–83 not undergoing the structural transition (Fig. 3B and D).

3.4. Effects of the G26R mutation on amyloid fibril formation of apoA-I 1–43 peptide

We next examined the effects of the G26R mutation on the fibril-forming propensity of the 1–43 peptide. As shown in Fig. 5A, the 1–43/G26R peptide exhibited much faster kinetics but lower final intensity for the development of ThT fluorescence compared to that of the 1–43 peptide, consistent with the finding that the G26R mutation enhances the fibrillation kinetics of the N-terminal 1–83 fragment [11]. Comparison of ANS binding showed a more rapid increase in ANS fluorescence for the 1–43/G26R peptide than that of the 1–43 peptide, indicating that the G26R mutation also enhances aggregation of the 1–43 segment (Fig. 5B). Much greater intensity reduction and more blue shift of WMF of Trp fluorescence for the 1–43/G26R peptide after incubation (Supplementary Fig. S4) suggest that the 1–43 and 1–43/G26R peptides differ in their tertiary/quaternary aggregate structure, possibly resulting in a different interaction of ThT. An AFM image of the 1–43/G26R peptide after incubation demonstrated the formation of straight fibrils resembling the morphology of fibrils by the 1–43 peptide (Fig. 5C). FTIR spectra of the 1–43/G26R peptide revealed the structural change to β-sheet structure after incubation similarly to the 1–43 peptide (Fig. 5D). These results indicate that the G26R mutation greatly facilitates the aggregation and fibril formation of the 1–43 segment.

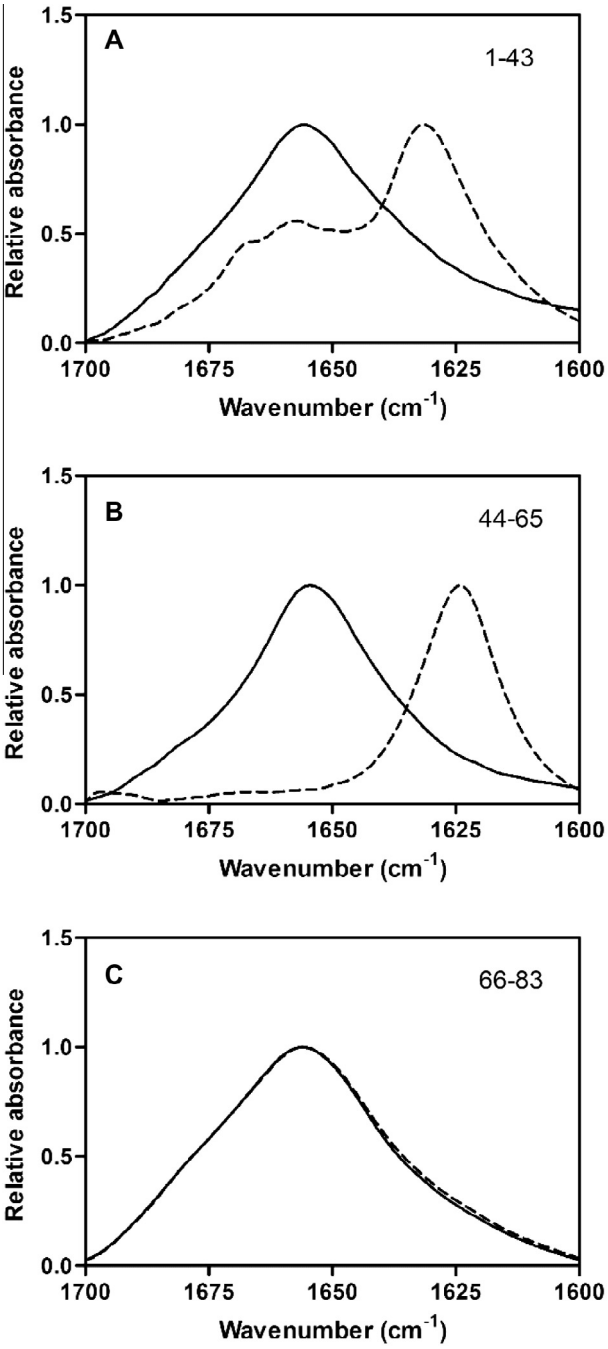

Fig. 4. ATR-FTIR spectra of apoA-I 1–43 (A), 44–65 (B), and 66–83 (C) peptides before (*solid line*) and after (*dashed line*) incubation for 144 h at pH 7.4.

4. Discussion

Our previous study demonstrated that the N-terminal 1–83 fragment of apoA-I has a strong propensity to form amyloid fibrils at physiological pH [11]. Theoretical prediction of the β-aggregation propensity of the N-terminal region in apoA-I indicates that residues 14–22 and 49–57 are the highly aggregation prone segments [9]. The X-ray crystal structure of a C-terminal truncated apoA-I variant [24] shows residues 44–55 being in an extended conformation, possibly providing a template for the intermolecular cross-β-sheet conformation [16]. Consistent with this, a peptide comprising residues 46–59 of apoA-I was shown to form amyloid-like fibrils, suggesting that this segment is responsible for the aggregation of apoA-I into amyloid fibrils [15].

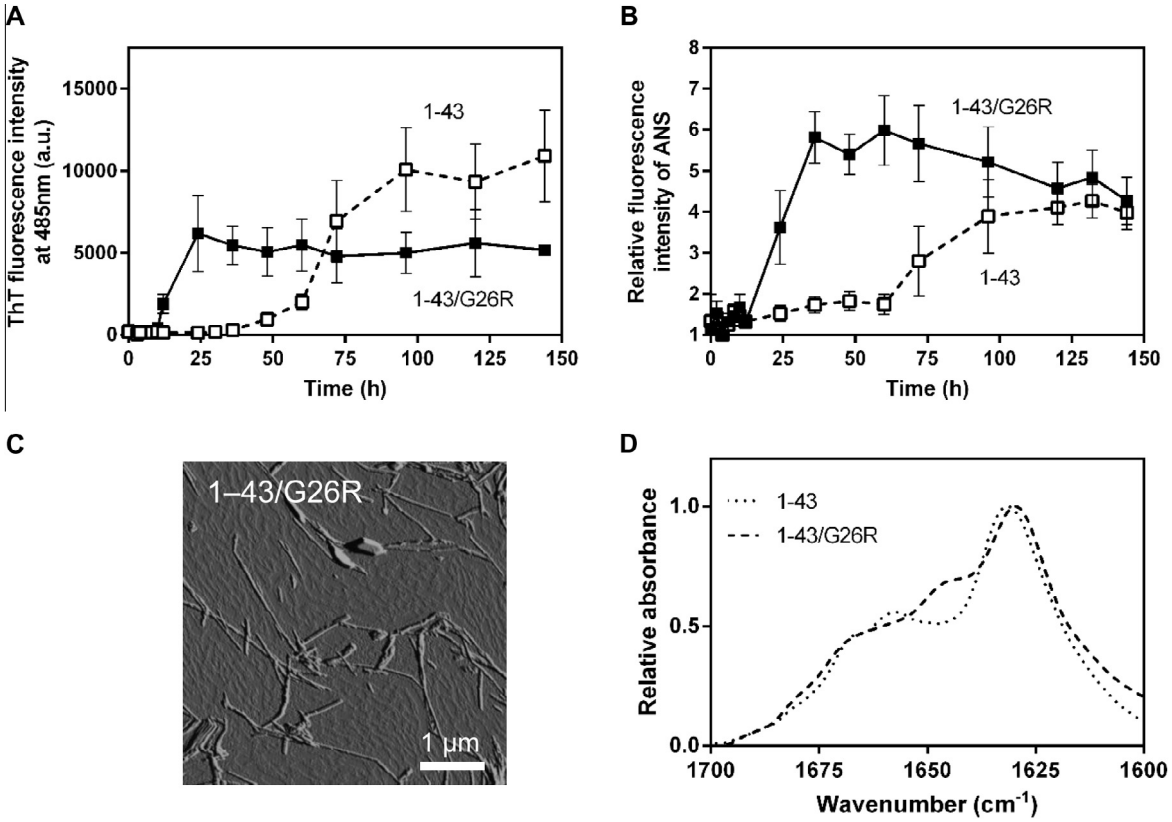

Fig. 5. Amyloid fibril formation of apoA-I 1–43/G26R peptide. ThT (A) and ANS (B) fluorescence of apoA-I 1–43/G26R (■, solid line) peptide over incubation time at pH 7.4. The results for apoA-I 1–43 peptide (□, dashed line) from Fig. 1 are also shown for comparison. (C) AFM image of apoA-I 1–43/G26R peptide after 144 h incubation at pH 7.4. Scale bar represents 1 μm. (D) ATR-FTIR spectrum of apoA-I 1–43/G26R peptide after incubation for 144 h at pH 7.4 (*dashed line*). The result for apoA-I 1–43 peptide (dotted line) from Fig. 4A is also shown for comparison.

In the present study, we demonstrated for the first time that the extreme N-terminal 1–43 segment has a strong propensity to form amyloid fibrils by using apoA-I fragment peptides corresponding to the N-terminal residues 1–43, 44–65 and 66–83. The 1–43 segment contains the first part of the most β-aggregation-prone regions (residues 14–22) in apoA-I, and indeed formed β-sheet-rich fibrils (Figs. 2A and 4A) with a great increase in ThT fluorescence (Fig. 1A) upon incubation. The fluorescence behavior of Trp-8 in the 1–43 peptide further demonstrates the conformational transition to the less solvent-exposed fibril structure (Fig. 3). The 44–65 peptide which contains the second part of the most β-aggregation-prone regions (residues 49–57) was also shown to have a propensity to form amyloid-like aggregates with the conformational transition to β-sheet structure (Figs. 1 and 4B), consistent with the previous report of the 46–59 peptide demonstrating the formation of amyloid-like fibrils that bind to ThT and contain cross-β structure [15]. The 66–83 peptide did not exhibit any ThT binding and conformational change at pH 7.4 (Figs. 1 and 4C) although it contains the predicted amyloid-forming sequence (residues 67–72) at acidic pH [25].

The first amyloidogenic segment (residues 14–22) in the N-terminal region contains very hydrophobic amino acids (LATVYVDVL), overlapping with the hydrophobic helix-forming region upon lipid binding of apoA-I [26,27]. The deletion of the extreme N-terminal residues 1–43 was shown to destabilize the N-terminal helix bundle structure and induce a large reduction in the enthalpy of lipid binding of full-length apoA-I [17,28], indicating critical roles of the 1–43 segment in the lipid-free conformation and lipid interaction of apoA-I. Taking into account the fact that the 1–43 peptide has a greater ability to bind to lipids than the 44–65 peptide [29], it is plausible that hydrophobic interactions play a role not only in lipid binding but also in fibril formation of the apoA-I peptides. To support this idea, substitution of Tyr-18 located at the center of the most hydrophobic region in residues 1–43 with a proline residue caused not only impaired lipid binding [29] but also strong inhibition of fibril formation of the 1–43 peptide (Supplementary Fig. S5).

Our previous study also demonstrated that the G26R point mutation greatly enhances the fibril formation of the N-terminal 1–83 fragment of apoA-I [11]. Similar to the case of the 1–83 fragment, the G26R mutation facilitates the aggregation and fibril formation kinetics of the 1–43 peptide (Fig. 5A and B), implying that the enhancing effect of the G26R mutation on the fibril formation comes from the local effect on the first amyloidogenic core region in apoA-I. Indeed, an electron paramagnetic resonance study indicated that the effect of the G26R mutation is likely to arise from the combination of losing the contribution of the native Gly residue in terminating β-strand propagation and the promotion of structural transition to a mixture of random coil and β-strand secondary structures by the substitution to an Arg residue [30].

In summary, the present results indicate that the 1–43 segment is highly amyloidogenic region within the N-terminal 1–83 residues of apoA-I, and that the G26R point mutation greatly enhances the fibril formation of this segment. Since the G26R mutation destabilizes the N-terminal helix bundle structure of apoA-I [11], it would expose the β-aggregation-prone region in residues 1–43 to facilitate protein aggregation. Thus, in addition to the proposed role of residues 46–59 in initiating aggregation and conversion into β-structure of apoA-I, the extreme N-terminal 1–43 residues appear to play a critical role in the development of amyloid fibrils by the N-terminal fragment of amyloidogenic apoA-I variants.

Acknowledgements

This work was supported by Grant-in-Aid for Scientific Research 25293006 and 25670014 from the Japan Society for the Promotion of Science. We thank Maki Nakamura for assistance of dynamic light scattering measurements. We are indebted to Dr. Michael C. Phillips (The Children's Hospital of Philadelphia) for his valuable comments.

Appendix A. Supplementary data

Supplementary data associated with this article can be found, in the online version, at http://dx.doi.org/10.1016/j.febslet.2013.11.031.

References

[1] Rosenson, R.S. et al. (2012) Cholesterol efflux and atheroprotection: advancing the concept of reverse cholesterol transport. Circulation 125, 1905–1919.
[2] Rader, D.J., Alexander, E.T., Weibel, G.L., Billheimer, J. and Rothblat, G.H. (2009) The role of reverse cholesterol transport in animals and humans and relationship to atherosclerosis. J. Lipid Res. 50 (Suppl.), S189–194.
[3] Sorci-Thomas, M.G. and Thomas, M.J. (2002) The effects of altered apolipoprotein A-I structure on plasma HDL concentration. Trends Cardiovasc. Med. 12, 121–128.
[4] Frank, P.G. and Marcel, Y.L. (2000) Apolipoprotein A-I: structure-function relationships. J. Lipid Res. 41, 853–872.
[5] Obici, L. et al. (1999) The new apolipoprotein A-I variant leu(174) -> Ser causes hereditary cardiac amyloidosis, and the amyloid fibrils are constituted by the 93-residue N-terminal polypeptide. Am. J. Pathol. 155, 695–702.
[6] de Sousa, M.M., Vital, C., Ostler, D., Fernandes, R., Pouget-Abadie, J., Carles, D. and Saraiva, M.J. (2000) Apolipoprotein AI and transthyretin as components of amyloid fibrils in a kindred with apoAI Leu178His amyloidosis. Am. J. Pathol. 156, 1911–1917.
[7] Andreola, A. et al. (2003) Conformational switching and fibrillogenesis in the amyloidogenic fragment of apolipoprotein a-I. J. Biol. Chem. 278, 2444–2451.
[8] Obici, L., Franceschini, G., Calabresi, L., Giorgetti, S., Stoppini, M., Merlini, G. and Bellotti, V. (2006) Structure, function and amyloidogenic propensity of apolipoprotein A-I. Amyloid 13, 191–205.
[9] Raimondi, S. et al. (2011) Effects of the known pathogenic mutations on the aggregation pathway of the amyloidogenic peptide of apolipoprotein A-I. J. Mol. Biol. 407, 465–476.
[10] Nichols, W.C., Dwulet, F.E., Liepnieks, J. and Benson, M.D. (1988) Variant apolipoprotein AI as a major constituent of a human hereditary amyloid. Biochem. Biophys. Res. Commun. 156, 762–768.
[11] Adachi, E. et al. (2013) Dual role of an N-terminal amyloidogenic mutation in apolipoprotein A-I: destabilization of helix bundle and enhancement of fibril formation. J. Biol. Chem. 288, 2848–2856.
[12] Rocken, C., Tautenhahn, J., Buhling, F., Sachwitz, D., Vockler, S., Goette, A. and Burger, T. (2006) Prevalence and pathology of amyloid in atherosclerotic arteries. Arterioscler. Thromb. Vasc. Biol. 26, 676–677.
[13] Wong, Y.Q., Binger, K.J., Howlett, G.J. and Griffin, M.D. (2010) Methionine oxidation induces amyloid fibril formation by full-length apolipoprotein A-I. Proc. Natl. Acad. Sci. USA 107, 1977–1982.
[14] Tartaglia, G.G., Pawar, A.P., Campioni, S., Dobson, C.M., Chiti, F. and Vendruscolo, M. (2008) Prediction of aggregation-prone regions in structured proteins. J. Mol. Biol. 380, 425–436.
[15] Wong, Y.Q., Binger, K.J., Howlett, G.J. and Griffin, M.D. (2012) Identification of an amyloid fibril forming peptide comprising residues 46–59 of apolipoprotein A-I. FEBS Lett. 586, 1754–1758.
[16] Gursky, O., Mei, X. and Atkinson, D. (2012) The crystal structure of the C-terminal truncated apolipoprotein A-I sheds new light on amyloid formation by the N-terminal fragment. Biochemistry 51, 10–18.
[17] Saito, H., Dhanasekaran, P., Nguyen, D., Holvoet, P., Lund-Katz, S. and Phillips, M.C. (2003) Domain structure and lipid interaction in human apolipoproteins A-I and E, a general model. J. Biol. Chem. 278, 23227–23232.
[18] Tanaka, M., Dhanasekaran, P., Nguyen, D., Ohta, S., Lund-Katz, S., Phillips, M.C. and Saito, H. (2006) Contributions of the N- and C-terminal helical segments to the lipid-free structure and lipid interaction of apolipoprotein A-I. Biochemistry 45, 10351–10358.
[19] Palgunachari, M.N., Mishra, V.K., Lund-Katz, S., Phillips, M.C., Adeyeye, S.O., Alluri, S., Anantharamaiah, G.M. and Segrest, J.P. (1996) Only the two end helixes of eight tandem amphipathic helical domains of human apo A-I have significant lipid affinity. Implications for HDL assembly. Arterioscler. Thromb. Vasc. Biol. 16, 328–338.
[20] Biancalana, M. and Koide, S. (2010) Molecular mechanism of Thioflavin-T binding to amyloid fibrils. Biochim. Biophys. Acta 1804, 1405–1412.
[21] Lindgren, M. and Hammarstrom, P. (2010) Amyloid oligomers: spectroscopic characterization of amyloidogenic protein states. FEBS J. 277, 1380–1388.
[22] Bolognesi, B. et al. (2010) ANS binding reveals common features of cytotoxic amyloid species. ACS Chem. Biol. 5, 735–740.
[23] Sarroukh, R., Goormaghtigh, E., Ruysschaert, J.M. and Raussens, V. (2013) ATR-FTIR: A "rejuvenated" tool to investigate amyloid proteins. Biochim. Biophys. Acta 1828, 2328–2338.
[24] Mei, X. and Atkinson, D. (2011) Crystal structure of C-terminal truncated apolipoprotein A-I reveals the assembly of high density lipoprotein (HDL) by dimerization. J. Biol. Chem. 286, 38570–38582.
[25] Lopez de la Paz, M. and Serrano, L. (2004) Sequence determinants of amyloid fibril formation. Proc. Natl. Acad. Sci. USA 101, 87–92.
[26] Saito, H., Lund-Katz, S. and Phillips, M.C. (2004) Contributions of domain structure and lipid interaction to the functionality of exchangeable human apolipoproteins. Prog. Lipid Res. 43, 350–380.
[27] Chetty, P.S., Mayne, L., Lund-Katz, S., Stranz, D., Englander, S.W. and Phillips, M.C. (2009) Helical structure and stability in human apolipoprotein A-I by hydrogen exchange and mass spectrometry. Proc. Natl. Acad. Sci. USA 106, 19005–19010.
[28] Saito, H., Dhanasekaran, P., Nguyen, D., Deridder, E., Holvoet, P., Lund-Katz, S. and Phillips, M.C. (2004) α-Helix formation is required for high affinity binding of human apolipoprotein A-I to lipids. J. Biol. Chem. 279, 20974–20981.
[29] Tanaka, M., Tanaka, T., Ohta, S., Kawakami, T., Konno, H., Akaji, K., Aimoto, S. and Saito, H. (2009) Evaluation of lipid-binding properties of the N-terminal helical segments in human apolipoprotein A-I using fragment peptides. J. Pept. Sci. 15, 36–42.
[30] Lagerstedt, J.O., Cavigiolio, G., Roberts, L.M., Hong, H.S., Jin, L.W., Fitzgerald, P.G., Oda, M.N. and Voss, J.C. (2007) Mapping the structural transition in an amyloidogenic apolipoprotein A-I. Biochemistry 46, 9693–9699.